

PopIII-star siblings in IZw18 and WRs in metal-poor galaxies unveiled from integral field spectroscopy

C. Kehrig¹, J.M. Vílchez¹, E. Pérez-Montero¹, J. Iglesias-Páramo^{1,2}, J. Brinchmann³, P.A. Crowther⁴, F. Durret⁵, D. Kunth⁵ & et al.

¹*Instituto de Astrofísica de Andalucía (IAA-CSIC), Spain*

²*Estación Experimental de Zonas Áridas (CSIC), Spain*

³*Leiden University, The Netherlands*

⁴*University of Sheffield, United Kingdom*

⁵*Institut d'Astrophysique de Paris, France*

Here we highlight our recent results from the IFS study of Mrk178, *the closest metal-poor WR galaxy*, and of IZw18, *the most metal-poor star-forming galaxy known in the local Universe*. The IFS data of Mrk178 show the importance of aperture effects on the search for WR features, and the extent to which physical variations in the ISM properties can be detected. Our IFS data of IZw18 reveal its entire nebular HeII λ 4686-emitting region, and indicate for the first time that peculiar, very hot (nearly) metal-free ionizing stars (called here *PopIII-star siblings*) might hold the key to the HeII-ionization in IZw18.

1 Introduction

Studying the WR content and radiative feedback from WRs in metal-poor star-forming (SF) galaxies is crucial to test evolutionary models for massive stars at low metallicity (Z), where the disagreement between observations and such models is stronger (e.g., Leitherer et al., 2014). In this context, we have initiated a program to investigate nearby low-Z WR galaxies using integral field spectroscopy (IFS). IFS has many advantages in a study of this kind, in comparison with long-slit spectroscopy (e.g., Kehrig et al., 2008; Pérez-Montero et al., 2011, 2013). By means of IFS one can find WRs where they were not detected before. Also, IFS is a powerful technique to probe and solve issues related with aperture effects, and allows a more precise spatial correlation between massive stars and nebular properties (e.g., Kehrig et al., 2008, 2013, hereafter K13). As a part of this program, we have obtained new IFS data of the low-Z galaxies Mrk178 and IZw18, published in K13 and Kehrig et al. (2015, hereafter K15), respectively. Below we summarize the main results from these two works.

2 IZw18: PopIII-star siblings as the source of HeII-ionization

We performed new IFS observations of IZw18 using the PMAS IFU (Roth et al., 2005) on the 3.5m telescope at CAHA (fig.1; K15). IZw18 is a nearby SF galaxy, well known for its extremely low $Z \sim (1/40) Z_{\odot}$ (e.g., Vílchez & Iglesias-Páramo, 1998), and it is considered an excellent local analog of primeval systems. Our IFS data reveal for the first time the entire nebular HeII λ 4686-emitting region (fig.2) and corresponding total HeII-ionizing photon flux [$Q(\text{HeII})_{\text{obs}}$] in IZw18. Narrow HeII emission in SF galaxies has been suggested to be mainly associ-

ated with photoionization from WRs, but WRs cannot satisfactorily explain the HeII-ionization in all cases, particularly at lowest metallicities where HeII emission is observed to be stronger (e.g., Guseva, Izotov, & Thuan, 2000; Kehrig, Telles, & Cuisinier, 2004; Shirazi & Brinchmann, 2012). Why is studying the formation of HeII emission relevant? HeII emission indicates the presence of high energy photons ($E \geq 54$ eV), and HeII-emitters are apparently more frequent among high-redshift (z) galaxies than for local objects (e.g., Kehrig et al., 2011; Cassata et al., 2013). Narrow HeII emission has been suggested as a good tracer of PopIII-stars (the first very hot metal-free stars) in high-z galaxies (e.g., Schaerer, 2003; Pallottini et al., 2015); these stars are believed to have contributed significantly to the reionization of the Universe, a challenging subject in contemporary cosmology. However, the origin of narrow HeII lines remains difficult to understand in many nearby SF galaxies/regions (e.g., Kehrig et al., 2011; Shirazi & Brinchmann, 2012). So before interpreting high-z HeII-emitters, it is crucial first to understand the formation of HeII emission at low redshift. IZw18, as the most metal-poor HeII-emitter in the local Universe, is an ideal object to perform this study.

Our observations combined with stellar model predictions point out that conventional excitation sources (e.g. single WRs, shocks, X-ray binaries) cannot convincingly explain the total $Q(\text{HeII})_{\text{obs}}$ derived for IZw18 (e.g., Meynet & Maeder, 2005; Crowther & Hadfield, 2006; Leitherer et al., 2014). Other mechanisms are probably also at work. If the HeII-ionization in IZw18 is due to stellar sources, these might be peculiar very hot stars. Based on models of very massive O stars (Kudritzki, 2002), ~ 10 -20 stars with $300 M_{\odot}$ at Z_{IZw18} [or lower, down to $Z \sim (1/100) Z_{\odot}$] can reproduce our total $Q(\text{HeII})_{\text{obs}}$ (see also Szécsi et al., 2015). However, the super-massive star scenario requires a cluster mass much higher than the mass of the IZw18 NW knot (where

the HeII region is located), and it would not be hard enough to explain the highest HeII/H β values observed. Also, stellar sources with 300 M $_{\odot}$ are not observed in IZw18 to date. Next, as an approximation of (nearly) metal-free stars in IZw18 – the so-called *PopIII-star siblings* – we compared our observations with models for rotating Z=0 stars (Yoon, Dierks, & Langer, 2012), which reproduce our data better: ~ 8 -10 of such stars with M $_{ini}$ =150 M $_{\odot}$ can explain the total Q(HeII) $_{obs}$ and the highest HeII/H β values observed. The PopIII-star sibling scenario, invoked for the first time in IZw18 by K15, goes in line with the reported metal-free gas pockets in the HI envelope near the IZw18 NW knot (Lebouteiller et al., 2013). These gas pockets could provide the raw material for making such *PopIII-star siblings*.

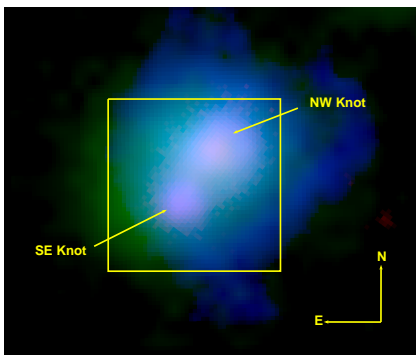


Fig. 1: Color-composite image of IZw18. The box represents the FOV (16" \times 16") of the PMAS IFU over the galaxy main body which hosts the NW and SE knots (Figure taken from K15).

3 Mrk178

In K13 we present the first optical IFS study of Mrk178, the closest metal-poor WR HII galaxy. IFS data of Mrk 178 were obtained with the INTEGRAL IFU at the 4.2m WHT. In this work we examine the spatial correlation between its WRs and the neighbouring ionized ISM. The strength of the broad WR features and its low metallicity ($\sim 1/10 Z_{\odot}$) make Mrk178 an intriguing object. We have detected the blue and red WR bumps in different locations across the FOV (~ 300 pc \times 230 pc) in Mrk178 (fig.3). The study of the WR content has been extended, for the first time, beyond its brightest SF knot (knot B in fig.3) uncovering new WR star clusters (knots A and C in fig.3). Using SMC/LMC template WRs (Crowther & Hadfield, 2006), we empirically estimate a minimum of ~ 20 WRs in our Mrk178 FOV, which is already higher than that currently found in the literature. Regarding the ISM abundances, localized N and He enrichment, spatially correlated with WRs from knot B, is suggested by our analysis. Nebular HeII λ 4686 emission is shown to be spatially

extended reaching well beyond the location of the WRs (fig.4). Shock ionization and X-ray binaries are unlikely to be significant ionizing mechanisms since Mrk178 is not detected in X-rays. The main excitation source of HeII in Mrk178 is still unknown.

From SDSS spectra of metal-poor WR galaxies, we found a too high EW(WR bump)/EW(H β) value for Mrk178, which is the most deviant point in the sample (fig.4). Using our IFU data, we showed that this curious behaviour is caused by aperture effects, which actually affect, to some degree, the EW(WR bump) measurements for all galaxies in Fig.4. Also, we demonstrated that using too large an aperture, the chance of detecting WR features decreases, and that WR signatures can escape detection depending on the distance of the object and on the aperture size. Thus, WR galaxy samples constructed on a single fiber/long-slit spectrum basis may be affected by systematic bias.

References

- Cassata P., et al., 2013, A&A, 556, A68
 Crowther P. A., Hadfield L. J., 2006, A&A, 449, 711
 Guseva N. G., Izotov Y. I., Thuan T. X., 2000, ApJ, 531, 776
 Kehrig C., Telles E., Cuisinier F., 2004, AJ, 128, 1141
 Kehrig C., Vílchez J. M., Sánchez S. F., Telles E., Pérez-Montero E., Martín-Gordón D., 2008, A&A, 477, 813
 Kehrig C., Oey M. S., Crowther P. A. et al., 2011, A&A, 526, A128
 Kehrig C., Pérez-Montero E., Vílchez J.M., et al., 2013, MNRAS, 432, 2731
 Kehrig C., Vílchez J. M., Pérez-Montero E., Iglesias-Páramo J., Brinchmann J., Kunth D., Durret F., Bayo F. M., 2015, ApJ, 801, L28
 Kudritzki R. P., 2002, ApJ, 577, 389
 Lebouteiller V., Heap S., Hubeny I., Kunth D., 2013, A&A, 553, A16
 Leitherer C., et al., 2014, ApJS, 212, 14
 Meynet G., Maeder A., 2005, A&A, 429, 581
 Pallottini, A., Ferrara, A., Pacucci, F., et al. 2015, MNRAS, 453, 2465
 Pérez-Montero E., et al., 2011, A&A, 532, A141
 Pérez-Montero E., Kehrig C., Brinchmann J., Vílchez J. M., Kunth D., Durret F., 2013, AdAst, 837, 392
 Roth M. M., et al., 2005, PASP, 117, 620
 Schaerer D., 2003, A&A, 397, 527
 Shirazi M., Brinchmann J., 2012, MNRAS, 421, 1043
 Szécsi, D., Langer, N., Yoon, S.-C., et al. 2015, A&A, 581, A15
 Vílchez J. M., Iglesias-Páramo J., 1998, ApJ, 508, 248
 Yoon S.-C., Dierks A., Langer N., 2012, A&A, 542, A113

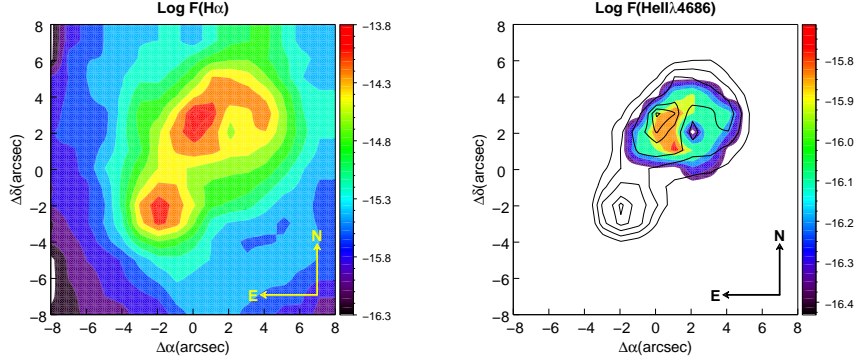


Fig. 2: IZw18: intensity maps of $H\alpha$ (left panel) and nebular $HeII\lambda 4686$ (right panel) in logarithmic scale; fluxes are in units of $\text{erg s}^{-1} \text{cm}^{-2}$. The maps are presented as color-filled contour plots (Figure taken from K15).

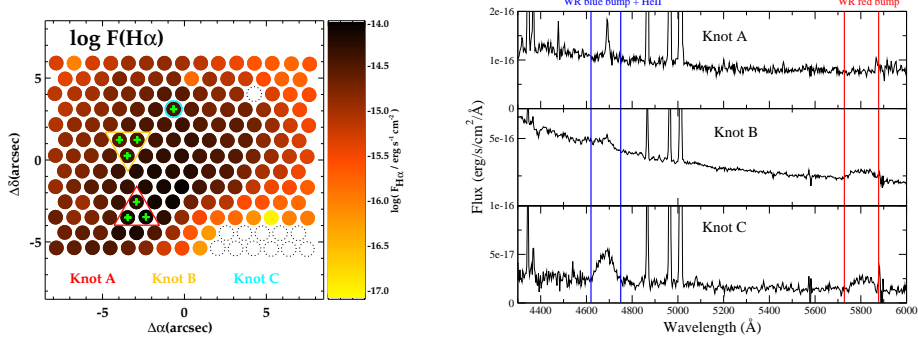


Fig. 3: Mrk178: intensity map of $H\alpha$ emission line (left panel) and integrated spectrum for the 3 knots in which WR features are detected (right panel). The spectral range for both blue and red WR bumps are marked (K13).

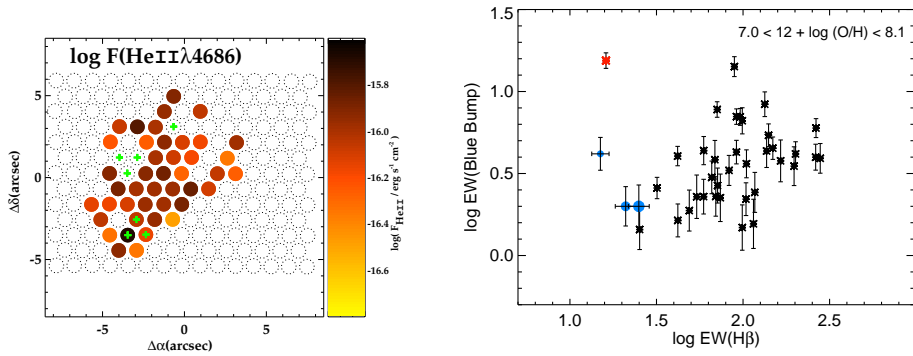


Fig. 4: Left panel: map of nebular $HeII\lambda 4686$ line; spaxels where we detect WR features are marked with green crosses. Right panel: $EW(\text{WR blue bump})$ vs $EW(H\beta)$. Asterisks show values from SDSS DR7 for metal-poor WR galaxies; the red one represents Mrk178. The three blue circles, from the smallest to the biggest one, represent the 5", 7" and 10" diameter apertures from our IFU data centered at the SDSS fiber of Mrk178 (K13).